Dissociative Double Ionization following Valence and Si:2p Core Level Photoexcitation of $SiCl_4$ in the Range 38−133 eV

Bong Hyun Boo,*,† Seung Min Park,‡ and Inosuke Koyano*,§

Department of Chemistry, Chungnam National University, Taejon 305-764, Korea, Center for Molecular Science, 373-1 Kusung-dong Yusung-gu, Taejon 305-701, Korea, Department of Chemistry, Kyung Hee University, Seoul 130-701, Korea, and the Department of Material Science, Himeji Institute of Technology, 1479-1 Kanaji, Kamigohri, Hyogo 678-12, Japan

Received: February 20, 1995; In Final Form: May 23, 1995⊗

The photoionization of $SiCl_4$ has been investigated in the valence and Si:2p inner-shell region using time-of-flight mass spectrometry and synchrotron radiation in the range 38−133 eV. Ion yields and branching ratios are reported for charged species arising from the dissociative photoionization processes. Various monocations such as Cl^+, Cl_2^+, and $SiCl_n^+$ ($n = 0-4$) are observed together with doubly charged species such as Si^{2+}, Cl^{2+}, and $SiCl^{2+}$. The photoion−photoion coincidence (PIPICO) technique has been employed to investigate a variety of dissociation processes *via* Coulomb explosion and to elucidate the dissociation mechanisms. Ion pairs of $Si^+ + Cl^+$ and $SiCl^+ + Cl^+$ are observed dominantly in the Si:2p edge. Variation of the ionic fragmentation as a function of photon energy is discussed in conjunction with the relevant electronic states.

Introduction

Ionic fragmentation of tetrachlorosilane ($SiCl_4$) has drawn a great deal of attention due to the growing interest in plasma deposition and light-stimulated chemical vapor deposition in the microelectronics industry. In recent years, dissociation processes following core level photoexcitation of silicon compounds with T_d symmetry such as SiH_4,[1] $Si(CH_3)_4$,[2] SiF_4,[3,4] and $SiCl_4$[5] have been current topics. All these studies were focused on dissociative double ionization following resonant core excitation in the vicinity of the Si:2p threshold.

Generally, double photoionization of gas molecules occurs when they absorb enough photon energy for two-electron ejection. Because of the Coulomb repulsion between two positive holes, the doubly charged parent ions are not particularly stable and tend to dissociate into their daughter ions.

In the present paper, we report the dissociative double ionization of $SiCl_4$ following valence and Si:2p core photoexcitation in the range 38−133 eV investigated by use of synchrotron radiation and photoelectron−photoion coincidence (PEPICO) and photoion−photoion coincidence (PIPICO) methods.

In contrast to excitation of valence electrons delocalized over the whole molecule, excitation of core electrons localized in a specific site on the molecules gives rise to quite different fragmentation patterns than observed in the valence excitation.[5-9] Variation of branching ratios for ions and PIPICO and of dissociation patterns with photon energy is discussed in conjunction with the relevant electronic state.

Experimental Section

The present experiments were performed using a time-of-flight (TOF) mass spectrometer coupled to a constant-deviation grazing incidence monochromator installed at the BL3A2 beam line of the ultraviolet synchrotron orbital radiation (UVSOR) facility in Okazaki. The design and construction of the apparatus have been described in detail elsewhere.[10,11] The time-of-flight mass spectrometer employs a drift tube of adjustable length to facilitate detection of metastable ions and to obtain better mass-resolved spectra. In addition, the mass detection angle can be varied by rotating the mass spectrometer in the plane perpendicular to the incident photon beam direction. For these experiments, a quasi-magic angle of 55° between the TOF axis and the photon polarization direction was used for the isotropic collection of the fragment ions. The TOF spectrometer is operated by time-correlated ion-counting techniques in two different modes: a photoelectron−photoion coincidence (PEPICO) mode and a photoion-photoion coincidence (PIPICO) mode. Flight-path lengths of 20, 40, and 80 cm were used in the present study. All the spectra shown here are for 20 cm. To operate the PEPICO mode, the start pulse for the time-to-amplitude converter (TAC) was provided by the photoelectron signal, sampled from the collision chamber in the opposite direction to the ion flight direction and perpendicular to the incident photon beam, and the stop pulse was provided by the photoion signal. The PIPICO mode was operated in the same way as the PEPICO mode. The start pulse for the TAC was provided by the lighter photoion signals, sampled from the TOF tube, and the stop pulse was provided by the heavier photoion signal. A thin optical filter of aluminum was used in the energy range below 68 eV for the elimination of higher order radiation. The slit width of the monochromator was 200 μm. The background pressure of the main chamber was $\approx 3 \times 10^{-9}$ Torr. When the tetrachlorosilane gas was introduced to the ionization chamber, the pressure in the main chamber was maintained at $\approx 7 \times 10^{-7}$ Torr. The $SiCl_4$ sample gas with a purity of 99.999 wt/wt % was purchased from Asahi Denka Kougyeou Co. and used without further purification. The TOF mass spectra confirmed its purity.

Results and Discussion

The total photoionization efficiency curve of $SiCl_4$ has one broad feature below 100 eV and four peaks at 105.0, 106.1, 110.6, and 121.4 eV near the Si:2p edge corresponding to A to D represented in Figure 1. The curve is quite similar to that observed previously in our laboratory.[5] These experimental peak positions are very close to four absorption bands at 104,

† Chungnam National University and Center for Molecular Science.
‡ Kyung Hee University.
§ Himeji Institute of Technology.
⊗ Abstract published in *Advance ACS Abstracts,* July 1, 1995.

0022-3654/95/2099-13362$09.00/0

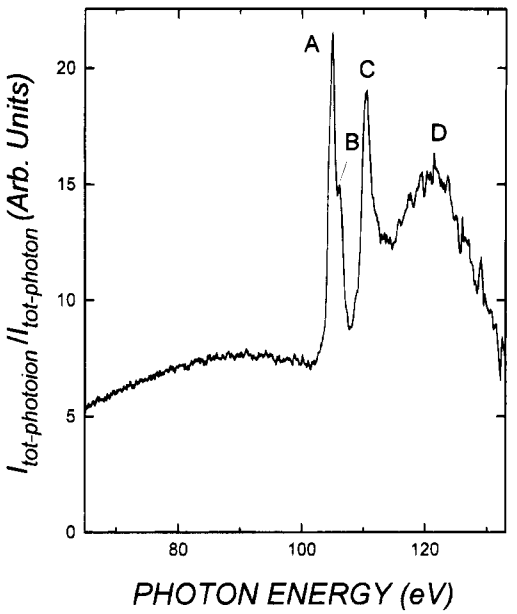

Figure 1. Total photoionization efficiency curve of $SiCl_4$ in the range 65−133 eV.

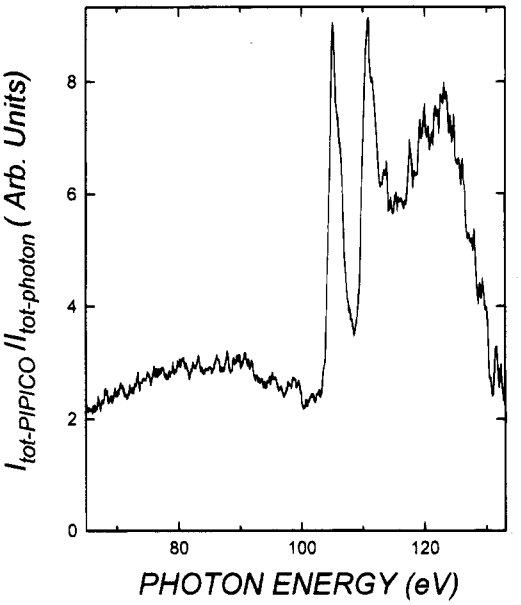

Figure 2. Total photoion−photoion coincidence efficiency curve of $SiCl_4$ in the range 65−133 eV.

TABLE 1: Electronic Configuration of $SiCl_4$[a]

orbital involved	symmetry and no. of electrons occupied
Cl 1s	$(1t_2)^6$, $(1a_1)^2$
Si 1s	$(2a_1)^2$
Cl 2s	$(2t_2)^6$, $(3a_1)^2$
Si 2s	$(4a_1)^2$
Cl 2p	$(5a_1)^2$, $(3t_2)^6$, $(1e)^4$, $(4t_2)^6$, $(1t_1)^6$
Si 2p	$(5t_2)^6$
inner-valence MO	$6a_1$(Cl 3s−Si 3s)^2, $6t_2$(Cl 3s−Si 3p)^6
outer-valence MO	$7a_1$(Si 3s−Cl 3p,3s)^2, $7t_2$(Si 3p−Cl 3p)^6
Cl 3p	$(2e)^4$, $(8t_2)^6$, $(2t_1)^6$

[a] Based on refs 14 and 25.

105.6, 110, and 124 eV, the values reported previously.[12] A broad and structureless feature below 100 eV is due to the valence single and double ionization *via* a nonresonant process. In a previous study, partial cross sections for the photoionization of the $7a_1$, $7t_2$, 2e, $8t_2$, and $2t_1$ valence orbitals in $SiCl_4$ were found to be small, in the range 38−80 eV.[13] The electronic configuration of $SiCl_4$ is represented in Table 1.

The first prominent peak starts to rise at 102.2 eV and then reaches a maximum at 105.0 eV in the total photoion intensity ($I_{tot\text{-}photoion}/I_{tot\text{-}photon}$), which is due to site-specific resonance photoexcitation of Si:2p to the $\sigma^*(8a_1)$ antibonding orbital. A small feature on the shoulder having a maximum at 106.1 eV may arise from excitation of Si:2p to the $\sigma^*(9t_2)$ orbital. These peak assignments are based on a previous molecular orbital calculation in which $8a_1$, $9t_2$, 4e, and $12t_2$ are found to be antibonding orbitals.[14] The Si:2p peak position can be more or less shifted due to the chemical environment surrounding the Si:2p core electron. It is accepted as a universal rule that the chemical shifts of photoelectron and Auger lines are linearly dependent on the averaged differences in Pauling's electronegativities to the nearest neighbors, $\Delta\bar{\chi}_P$.[15]

Friedrich *et al.* proposed that the experimental position of the peak for the photoexcitation of Si:$2p_{3/2}$ to $\sigma^*(a_1)$ in SiF_4 is 106.13 ± 0.2 eV.[16] This value is a little higher than the maximum in the total photoionization efficiency curve, reflecting the electronegativity difference between F and Cl atoms.

The excitation of a Si:2p electron into antibonding orbitals can lead to resonant Auger processes that leave the $SiCl_4$ molecules with two holes in the valence orbitals. By the presence of one electron in the antibonding orbital or the continuum, the Si:2p excited state species decays *via* double-resonance Auger processes to form doubly charged species.

Chlorine lone pairs with the symmetries of e and t_1 do not contribute directly to the silicon spectrum, but the presence of a Si:2p hole increases the valence electron population in the a_1 and t_2 orbitals *via* the back-donation of the chlorine lone pair electrons to Si:2p. On the basis of Mulliken population analysis, the total electron population on the silicon atom increases.[17] This effect can increase the rate for the Auger processes, giving rise to the double and/or triple vacancies.[18]

Figure 2 shows the variation of the total PIPICO intensity ($I_{tot\text{-}PIPICO}/I_{tot\text{-}photon}$) with photon beam energy. Notice that the curve was obtained by recording PIPICO count rates and photon count rates simultaneously while the photon wavelength was scanned and then by dividing the recorded PIPICO count rates by the recorded photon count rates. When the PIPICO count rates are measured, the coincidence time range (gate width in TAC) was set to be 0−5 μs. That this is the correct time range for collecting all PIPICO signals relevant to the fragmentation of doubly or multiply charged precursor ions is seen from a TOF mass spectrum, such as that shown in Figure 3, which indicates that the TOF difference between any pairs of the observed ions falls in this time range.

At energies near the Si:2p edge, the total PIPICO efficiency curve shown in Figure 2 is quite similar to the total photoionization efficiency curve. This means that the photoabsorption in the Si:2p excitation region almost always leads to dissociative double ionization. The ratios of the total PIPICO efficiencies to the total ion efficiencies are smaller in the valence excitation region than in the Si:2p excitation region. This indicates that the valence excitation/ionization partially leads to dissociative single ionization. Figure 2 also shows clear peaks at 105.0, 110.9, and 123.1 eV corresponding to the A, C, and D peaks in Figure 1. It is presumed that the B peak observed in Figure 1 is smeared in the A peak in Figure 2.

In Figure 2, we also observe a sudden rise of the PIPICO signal at 103.1 eV. This onset corresponds to the threshold for the dissociative double ionization following the Si:2p core excitation to the $8a_1$ antibonding orbital.

The C peak in Figure 1 having a maximum at 110.6 eV in Figure 1 and at 110.9 eV in Figure 2 may correspond to the photoexcitation of Si:2p to the 4e antibonding orbital[14] and/or

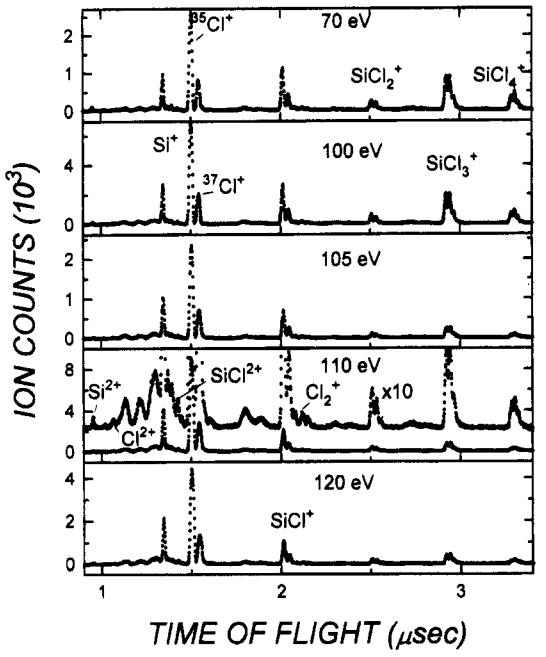

Figure 3. Photoelectron−photoion coincidence (mass) spectra of $SiCl_4$ measured at various photon energies.

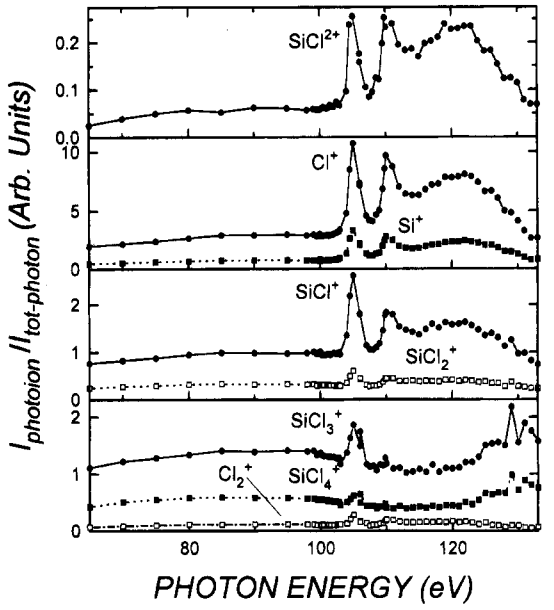

Figure 4. Partial photoion yield spectra of $SiCl_4$ in the range 65−133 eV. The spectral intensities ($I_{photoion}/I_{tot\text{-}photon}$) are presented on the same relative intensity scale.

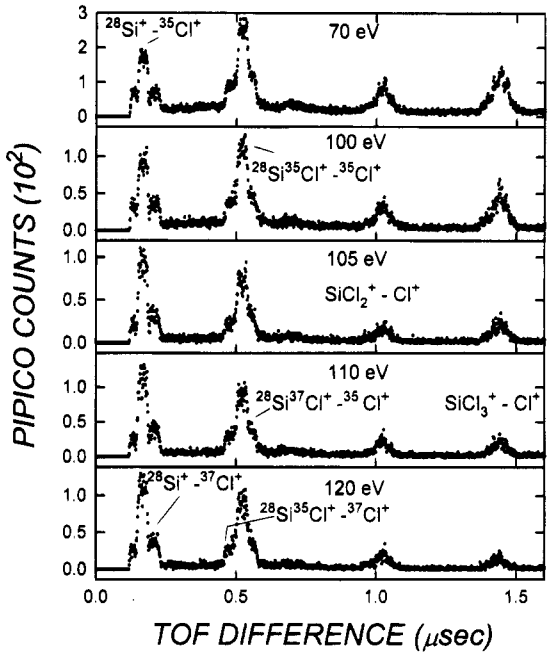

Figure 5. Photoion−photoion coincidence (PIPICO) spectra of $SiCl_4$ measured at various photon energies.

the Rydberg orbitals such as 4s, 3d, 4d, 5s, etc., converging to the Si:2p photoionization threshold. Contrary to expectation, the peak position of 110.6 eV is a little higher than the maximum value of 110 eV in the photoabsorption spectrum[12] and the adiabatic ionization potentials of the Si:$2p_{3/2}$ core level of $SiCl_4$, 110.18,[19] 110.17,[20,21] and 110.25 eV.[22]

The broad D peak having a maximum at 121.4 eV in Figure 1 and 123.1 eV in Figure 2 may be due to electronic excitation of Si:2p to the $12t_2$ antibonding orbital[14] and/or quasi-bound unoccupied orbitals supported by a potential energy barrier created by the strong electronegative ligands.[23,24] In the potential well, the excited electron could be backscattered by the Cl ligands, which gives rise to resonances above the threshold. This shape resonance has also been observed in the photoabsorption of SiF_4.[16]

Typical examples of TOF mass spectra of $SiCl_4$ taken by excitations at 70, 100, 105, 110, and 120 eV in the PEPICO mode are shown in Figure 3. In contrast to those of the dissociative double ionization of SiF_4,[3,4] doubly charged species of the dissociative double ionization of $SiCl_4$ have very low intensities.

Notice that as described in the Experimental Section, the PEPICO mode utilizes ion signals detected in the MCP as the stop pulse for the TAC. This results in mass discrimination for heavier ions being formed in a given molecule. But this mass discrimination effect is found to be negligibly small. The ratio of the total PIPICO intensity to the total photoionization intensity is as small as (1.99 ± 0.67) and (1.09 ± 0.19)% below and above the Si:2p excitation region, respectively. In the PEPICO measurements, the probability of detecting an ion pair altogether formed *via* fragmentation of a given doubly charged precursor is found to be as small as 1−2%.

The PEPICO (mass) spectra taken in the Si:2p excitation region (105, 110, and 120 eV in Figure 3) show that the intensities for Si^+ and Cl^+ ions are enhanced while those for $SiCl_3^+$ and $SiCl_4^+$ ions are diminished. The dramatic change in the ion count ratios corresponds to Coulomb explosion decomposition of $SiCl_4$.

As shown in Figure 3, the excitations to $8a_1$ and $9t_2$ (around 105 eV), to Rydberg orbitals or the continuum (around 110 eV), and to the $12t_2$ antibonding orbital and/or quasi-bound unoccupied orbitals (around 120 eV) exhibit similar fragmentation behaviors due to a strong valence character.

The variations of the individual ion intensities with the photon energy are exhibited in Figure 4. The energy dependence of the Si^{2+} and Cl^{2+} ion intensities is not shown due to their quite low intensities. The sum of the intensities for all the ions indicated in Figure 4 equals the total of the photoion intensities displayed in Figure 1. We can show the individual ion efficiency data only in the range 65−133 eV, displayed in Figure 4, due to the limited range covered by one grating. In Figure 4, all the ion intensities start to rise from ≈100 eV, showing two obvious humps in the discrete excitation region 100−120 eV.

We show in Figure 5 the PIPICO spectra in the valence excitation region (70, 100 eV), in the core excitation region (105 eV), near the threshold (110 eV), and above the edge (115

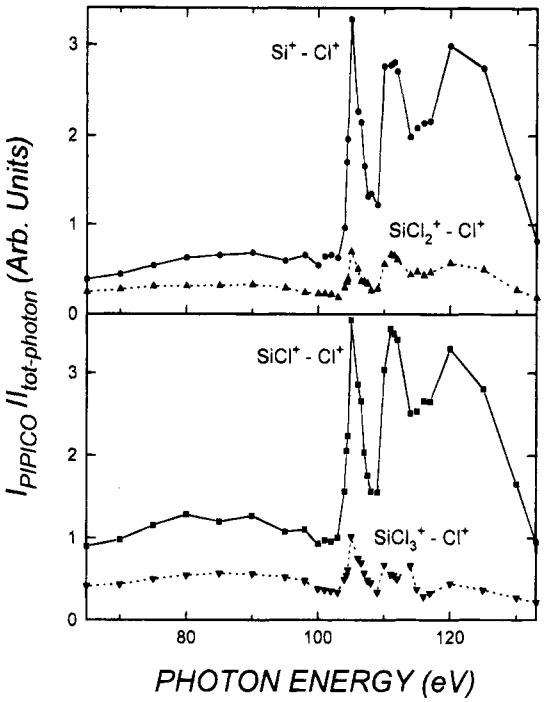

Figure 6. Photon energy dependence of the ion pairs detected by the PIPICO method. The spectral intensities ($I_{PIPICO}/I_{tot\text{-}photon}$) are presented on the same relative intensity scale.

eV). In the valence excitation region, ion pairs of $Cl^+-SiCl_n^+$ ($n = 2-3$) are seen abundantly. Contrary to expectations, an ion pair of Cl^+-Cl^+ is not seen at very short time-of-flight differences. This fact is contrary to the observation that a single pair of F^+-F^+ is found in the core excitation of SiF_4.[3] At the energies for discrete excitation, the PIPICO counts for the ion pairs of $SiCl_2^+-Cl^+$ and $SiCl_3^+-Cl^+$ are found to dip. The energetics of the fragmentation patterns are shown in the variation of the PIPICO intensities with the photon energies (Figure 6). It is noticed that the sum of the intensities for all the ion pairs indicated in Figure 6 is equal to the total PIPICO intensities exhibited in Figure 2. It is shown that the PIPICO intensities for Si^+-Cl^+ and $SiCl^+-Cl^+$ are the major contribution to the total PIPICO intensities. The three large peaks for Si^+-Cl^+ and $SiCl^+-Cl^+$ seen in Figure 6 correspond to an increase of the photoabsorption cross section of $SiCl_4$. This is further discussed below.

We show in Scheme 1 the dissociation behavior of the possible doubly charged precursor of $SiCl_4^{2+}$ formed *via* core excitation.

SCHEME 1

$$SiCl_4 + h\nu \rightarrow SiCl_4^*$$

[Si:2p excitation to antibonding orbitals]

$$SiCl_4^* \rightarrow SiCl_4^{2+*} + 2e$$

$$SiCl_4^{2+*} \rightarrow Cl^+ + SiCl_n^+ \ (n = 0-3) + np$$

$$\rightarrow SiCl_n^{2+} \ (n = 0, 1) + np$$

$$\rightarrow Cl_2^+ + SiCl_n^+ \ (n = 0-2) + np$$

$$\rightarrow Cl^{2+} + np$$

where np denotes neutral products.

It is of interest to clarify why the photoexcitation to a discrete orbital will lead to a doubly ionized species, process 1.

$$SiCl_4^* \rightarrow SiCl_4^{2+*} + 2e \quad (1)$$

Double-resonant Auger processes and two-step autoionization may be responsible for the formation of the doubly charged species. It is noticed that these relaxation mechanisms involving the core hole state are not clarified using only our simple PEPICO and PIPICO experiments, but the high yields of the ion-pair formation of $Cl^+-SiCl_n^+$ ($n = 0-3$) and the tendency to screen the core hole imply that the core hole state having an excited configuration such as $(Si:2p)^{-1}(valence, Si)^1$ may be relaxed by the Auger process as shown in reaction 2

$$(Si:2p)^{-1}(valence, Si)^1 \rightarrow (valence)^{-2}(ligand)^{-1}(valence, Si)^1 + 2e \quad (2)$$

where the (valence, Si) orbital refers to an unoccupied orbital with a significant atomic orbital localized on the silicon site. This implication is based on a previous photoelectron and Auger spectroscopic study of SiF_4 in which the core-excited molecule decays mostly by double-resonant Auger process and to a small extent by a double autoionization.[25] The presence of the hole in the ligand orbitals shown in eq 2 is based on the findings of the Cl^+ ion in the PEPICO mode and the $Cl^+-SiCl_n^+$ ($n = 0,1$) ion pairs in the PIPICO mode predominantly. In a photoion spectroscopic study of Ar, Hayaishi *et al.* argued that two-step autoionization shown below in eqs 3 and 4 seems more likely than shake-off as the reason for the formation of Ar^{2+} ions below the Ar:2p ionization limit.[26]

$$Ar\ 2p^{-1}5d \rightarrow Ar^+\ 3p^{-2}(^1D)6d + e_1 \quad (3)$$

$$Ar^+\ 3p^{-2}(^1D)6d \rightarrow Ar^{2+}\ 3p^{-2}(^3P) + e_2 \quad (4)$$

In the PIPICO spectroscopic study of $Si(CH_3)_4$, Morin *et al.* proposed that the double-resonant Auger process is more important than the direct double ionization below the Si:2p edge.[2] Souza *et al.* proposed in a photoelectron and Auger spectroscopy of SiH_4 that a very fast dissociation pathway involving eq 5 occurs in addition to autoionization and resonant Auger processes in the vicinity of the Si:2p edge.[1]

$$SiH_4^* \rightarrow SiH_3^* + H \rightarrow SiH_3^{+*} + e \ (\text{or } SiH_3^+ + e) \quad (5)$$

The ion branching ratios for Si^+ and Cl^+ show an energy dependence similar to the total photoionization efficiency, but the magnitude of the ratio (I_{Cl^+}/I_{Si^+}) changes from about 5.43 ± 0.73 in the range 38−50 eV to 3.68 ± 0.34 in the range 50−133 eV. This indicates that in the fragmentation of doubly charged species Si^+ plays a minor role as a counterpart of Cl^+ even in the Si:2p edge.

We show in Figure 7 the ion branching ratios as a function of the photon energy in the wider range 38−133 eV. Note that, at a given energy, the value for the $I_{photoion}/I_{tot\text{-}photon}$ is derived by multiplying the value for the $I_{tot\text{-}photoion}/I_{tot\text{-}photon}$ to the value for the ion branching ratio displayed in Figure 7. It is shown that the obvious features for Si^+ and Cl^+ in the Si:2p region are correlated with the declines in the ion branching ratios for $SiCl_n^+$ ($n = 2-4$). The ion branching ratio of $SiCl^+$ increases with increasing energy, approaching a maximum around 46 eV, and then falls off. The falloff is compensated by the rise in the ion branching ratios of Si^+ and Cl^+. Similar behaviors are also observed in the PIPICO ratio as shown in Figure 8. In the range 38−46 eV, it is clearly seen that the PIPICO signals due to $Cl^+ + SiCl_3^+$ and $Cl^+ + SiCl^+$ are mutually compensated. This implies that $SiCl_3^+$ further dissociates into $SiCl^+$ and neutral

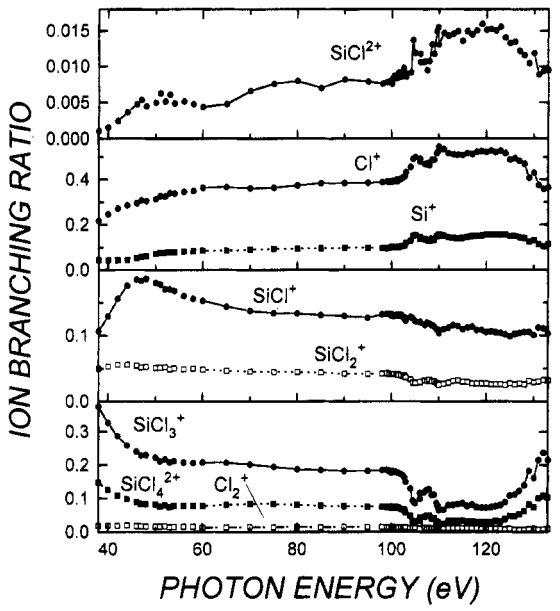

Figure 7. Ratios of integrated intensities of ion peaks in the TOF mass spectrum to total photoion intensity ($I_{photoion}/I_{tot\text{-}photoion}$) in $SiCl_4$ as a function of photon energy.

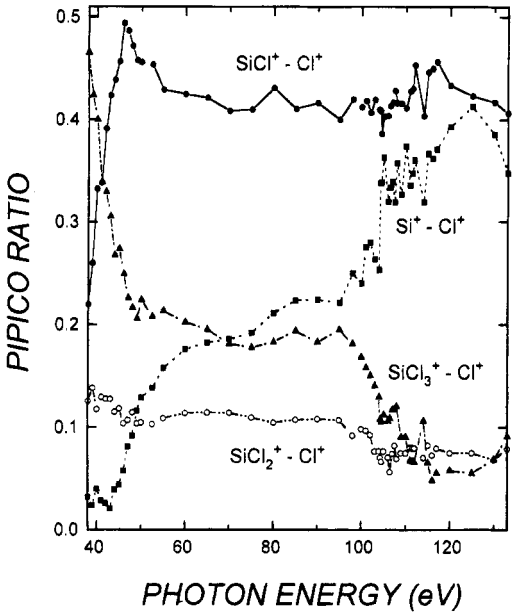

Figure 8. Ratios of integrated intensities of $Cl^+-SiCl_n^+$ ($n = 0-3$) ion pairs in the PIPICO spectrum to total double-photoionization ($I_{PIPICO}/I_{tot\text{-}PIPICO}$) in $SiCl_4$ as a function of photon energy.

fragments in the range. At higher energies ranging from 47 to 60 eV, some of the $SiCl^+$ ions further dissociate into $Si^+ + Cl$.

The variation of the ion intensity of Cl_2^+ with the photon energy shows small features in the Si:2p region, but the mechanism for the formation of the ion is unknown.

Why then does $SiCl_3^+$ tend to dissociate mostly into $SiCl^+ + Cl_2$ rather than $SiCl_2^+ + Cl$? In the ground state, $SiCl^+$ may have a closed-shell structure of $^1\Sigma^+$ while $SiCl_2^+$ has an unpaired electron on the Si center probably with an electronic structure of $^2A_1$. The presence of an unpaired electron on that position may weaken the $SiCl^+-Cl$ bond, as reflected from the low bond energies, $D°(SiCl^+-Cl) = 36 \pm 3$ kcal/mol, the value based on the thermochemical data listed in Table 2. It is noted here that the enthalpies of formation of various ionic species are derived by using the appearance potentials for $SiCl^+$,[27] $SiCl_2^+$,[27] $SiCl_3^+$,[28] and $SiCl_4^+$.[28,29] From the data, $D°(SiCl_3^+-Cl)$ is calculated to be as low as 15 ± 4 kcal/mol. On the contrary,

TABLE 2: Standard Enthalpies of Formation for Various Species at 298 K[a]

bond	$\Delta_f H^0$ (kcal/mol)
Cl	28.992 (0.002)
Cl^+	329.57 (0.46)[b]
$SiCl_4$	−158.40 (0.31)
Si^+	297.0 (1)
$SiCl^+$	198.9 (2.3)[c]
$SiCl_2^+$	191.9 (2.3)[c]
$SiCl_3^+$	104.7 (2.3)[d]
$SiCl_4^+$	118.2 (3.0)[e]

[a] All values except where noted are from Chase, M. W., Jr.; *et al. J. Phys. Chem. Ref. Data* **1985**, *14*, supplement 1 (JANAF Thermochemical Tables). This reference uses the thermal electron convention. Thus, ion heats of formation are 1.48 kcal/mol larger than values which do not include the heat of the electron. Uncertainties are in parentheses. [b] Derived using the ionization potential for Cl^+ ($^3P_2$) [De Leeuw, D. M.; Mooyman, R.; De Lange, C. A. *Chem. Phys. Lett.* **1978**, *54*, 231. Kimura, K.; Yamazaki, T.; Achiba, Y. *Chem. Phys. Lett.* **1978**, *58*, 104]. [c] Derived using the appearance potentials for $SiCl_n^+$ ($n = 1,2$) (ref 27). [d] Derived using the appearance potential for $SiCl_3^+$ (ref 28). [e] Derived using the ionization potential for $SiCl_4$ (refs 28 and 29).

SCHEME 2

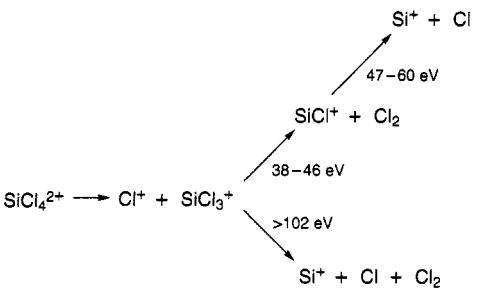

$D°(Si^+-Cl)$ and $D°(SiCl_2^+-Cl)$ are calculated to be as high as 127.1 ± 3 and 116.2 ± 3 kcal/mol, respectively.

Among the various channels for dissociation of $SiCl_n^+$ ($n = 2-4$) into Si^+ and neutral fragments in the Si:2p region, $SiCl_3^+$ plays a major role as a precursor for formation of Si^+. This interpretation is also verified by elucidating the PIPICO spectrum shown in Figure 8. The increase of the PIPICO ratio for $Cl^+ + Si^+$ in the range above 95 eV is almost compensated by the decrease of $Cl^+ + SiCl_3^+$. The major dissociation behavior of $SiCl_3^+$ in the two energy regions is summarized in Scheme 2, which accounts for the dissociation behavior of singly charged ions such as $SiCl_3^+$ and $SiCl^+$.

It is noted that the energy ranges for which the specific fragmentations occur are described in Scheme 2.

Conclusions

The Si:2p core excitations to antibonding orbitals have led to mostly double ionization favoring the spectator transition as observed in Si:2p core excitation in the molecule SiF_4. The double-photoionization threshold of $SiCl_4$, 103.0 eV, is much lower than the adiabatic ionization potential (110.2 eV) of the $Si:2p_{3/2}$ core level of $SiCl_4$. The clear features in the ion intensities of Cl^+ and $SiCl_n^+$ ($n = 0, 2-4$) are observed in the excitation ranges $100 < E < 115$ eV, which supports the occurrence of the double-resonant Auger processes involving the photoexcitation of Si:2p to the discrete levels of the $8a_1$, $9t_2$, 4e, and $12t_2$.

Acknowledgment. We wish to thank the members of the UVSOR facility for their valuable help during the course of the experiments. This work was partially supported by the Pohang Light Source, Pohang, Korea, through a visiting scientist

research program, by the Center for Molecular Science, Taejon, Korea, and from the Basic Science Research Institute Program, Ministry of Education, Korea, 1995−96 (B.H.B., Project No. BSRI-95-3432; S.M.P., BSRI-95-9401).

References and Notes

(1) de Souza, G. G. B.; Morin, P.; Nenner, I. *Phys. Rev. A* **1986**, *34*, 4770.
(2) Morin, P.; de Souza, G. G. B.; Nenner, I.; Lablanquie, P. *Phys. Rev. Lett.* **1986**, *56*, 131.
(3) Lablanquie, P.; Souza, A. C. A.; de Souza, G. G. B.; Morin, P.; Nenner, I. *J. Chem. Phys.* **1989**, *90*, 7078.
(4) Imamura, T.; Brion, C. E.; Koyano, I.; Ibuki, T.; Masuoka, T. *J. Chem. Phys.* **1991**, *94*, 4936.
(5) Nagaoka, S.; Oshita, J.; Ishikawa, M.; Masuoka, T.; Koyano, I. *J. Phys. Chem.* **1993**, *97*, 1488.
(6) Nagaoka, S.; Koyano, I.; Imamura, T.; Masuoka, T. *Appl. Organomet. Chem.* **1991**, 5, 269.
(7) Nagaoka, S.; Koyano, I.; Masuoka, T. *Phys. Scr.* **1990**, *41*, 472.
(8) Nagaoka, S.; Suzuki, S.; Nagashima, U.; Imamura, T.; Koyano, I. *J. Phys. Chem.* **1990**, *94*, 2283.
(9) Boo, B. H.; Lee, S. Y.; Koyano, I.; Masuoka, T. To be submitted for publication.
(10) Masuoka, T.; Horigome, T.; Koyano, I. *Rev. Sci. Instrum.* **1989**, *60*, 2179.
(11) Ishiguro, E.; Suzuki, M.; Yamazaki, M.; Nakamura, E.; Sakai, K.; Matsudo, O.; Mitsutani, N.; Fukui, K.; Watanabe, M. *Rev. Sci. Instrum.* **1989**, *60*, 2105.
(12) Zimkina, T. M.; Vinogradov, A. S. *J. Phys. (Paris) Colloq.* **1971**, *32*, C4-3.
(13) Carlson, T. A.; Fahlman, A.; Krause, M. O.; Whitley, T. A.; Grimm, F. A.; Piancastelli, M. N.; Taylor, J. W. *J. Chem. Phys.* **1986**, *84*, 641.
(14) Ishikawa, H.; Fujima, K.; Adachi, H.; Miyauchi, E.; Fujii, T. *J. Chem. Phys.* **1991**, *94*, 6740.
(15) Streubel, P.; Franke, R.; Chassé, Th.; Fellenberg, R.; Szargan, R. *J. Electron Spectrosc. Relat. Phenom.* **1991**, *57*, 1.
(16) Friedrich, H.; Pittel, B.; Rabe, P.; Schwarz, W. H. E.; Sonntag, B. *J. Phys. B: At. Mol. Opt. Phys.* **1980**, *13*, 25.
(17) Larkins, F. P.; McColl, J.; Chelkowska E. Z. *J. Electron. Spectrosc. Relat. Phenom.* **1994**, *67*, 275.
(18) McColl, J.; Larkins, F. P. *Chem. Phys. Lett.* **1992**, *196*, 343.
(19) Bozek, J. D.; Bancroft, G. M.; Tan, K. H. *Phys. Rev. A* **1991**, *43*, 3597.
(20) Kelfve, P.; Blomster, B.; Siegbahn, H.; Siegbahn, K.; Sanhueza, E.; Gosinski, O. *Phys. Scr.* **1980**, *21*, 75.
(21) Drake, J. E.; Riddle, C.; Coatsworth, L. *Can. J. Chem.* **1975**, *53*, 3602.
(22) Perry, W. B.; Jolly, W. L. *Inorg. Chem.* **1974**, *13*, 1211.
(23) Dehmer, J. L. *J. Chem. Phys.* **1972**, *56*, 4496.
(24) Tse, J. S.; Liu, Z. F.; Bozek, J. D.; Bancroft, G. M. *Phys. Rev. A* **1989**, *39*, 1791.
(25) de Souza, G. G. B.; Morin, P.; Nenner, I. *J. Chem. Phys.* **1989**, *90*, 7071.
(26) Hayaishi, T.; Murakami, E.; Yagishita, A.; Foike, F.; Morioka, Y.; Hansen J. E. *J. Phys. B: At. Mol. Opt. Phys.* **1988**, *21*, 3203.
(27) Ihle, H. R.; Wu, C. H.; Miletic, M.; Zmbov, K. F. *Adv. Mass Spectrom.* **1978**, *7A*, 670.
(28) Potzinger, P.; Ritter, A.; Krause, J. *Z. Naturforsch.* **1975**, *30a*, 347.
(29) Frost, D. C.; Herring, F. G.; Katrib, A.; McLean, R. A. N.; Drake, J. E.; Westwood, N. P. C. *Chem. Phys. Lett.* **1971**, *10*, 347.

JP950489W